Heliyon 11 (2025) e41789

Contents lists available at ScienceDirect

Heliyon

journal homepage: www.cell.com/heliyon

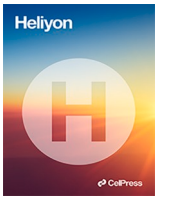

Research article

Nuclear factor I-C regulates intramembranous bone formation via control of FGF signalling

Jieun Lee [a], Joo-Cheol Park [b,d], Heung-Joong Kim [c], Hyun Sook Bae [a,**], Dong-Seol Lee [b,d,*]

[a] Department of Oral Hygiene, Namseoul University, Cheonan, Republic of Korea
[b] Department of Oral Histology-Developmental Biology, School of Dentistry and Dental Research Institute, Seoul National University, Seoul, Republic of Korea
[c] Department of Anatomy and Orofacial Development School of Dentistry Chosun University, Dong-gu, Gwangju, Republic of Korea
[d] Regenerative Dental Medicine R and D Center, Hysensbio Co., Ltd., Seoul, Republic of Korea

ARTICLE INFO

Keywords:
Nuclear factor I-C (NFI-C)
Fibroblast growth factor receptor 1 (FGFR1)
Osteogenic progenitor cells
Proliferation
Osteoblast differentiation

ABSTRACT

Our previous studies indicate that NFI-C is essential for tooth root development and endochondral ossification. However, its exact role in calvarial intramembranous bone formation remains unclear. In this study, we demonstrate that the disruption of the *Nfic* gene leads to defects in intramembranous bone formation, characterized by decreased osteogenic proliferative activity and reduced osteoblast differentiation during postnatal osteogenesis. Additionally, *Nfic*-deficient mice exhibited incomplete suture closure, although *Nfic* disruption did not affect prenatal calvarial bone development. We found that the expression levels of Fgfr1 and Fgfr2 were reduced in the primary calvarial mesenchymal cells of *Nfic*-deficient mice. In contrast, NFI-C overexpression in human bone marrow stromal cells (hBMSCs) significantly increased the expression of these factors. Furthermore, *NFI-C* regulates *FGFR1* expression by directly binding to its promoter. These results indicate that NFI-C is crucial in regulating calvarial bone formation and suture closure by controlling Fgfr1 expression and cellular proliferation.

1. Introduction

The skull consists of the calvarial bone, craniofacial bone, and cranial base [1]. The calvarial bone primarily includes a significant portion of the frontal bone, most of the two parietal bones, and smaller sections of the temporal and occipital bones [2]. Cranial sutures are essential in the calvarial bone's development, growth, and maintenance. The suture also plays an essential function in preventing premature bone separation of the calvarial bone during the growth process [3]. Craniosynostosis can occur if the cranial suture contains the skeletal stem and progenitor cells and does not maintain patency, and premature fusion occurs [4,5]. Therefore, the osteoblast progenitor cells within the suture need to undergo appropriate proliferation and maintain good differentiation potential to support normal skull development and formation.

Fibroblast growth factors (FGFs) and fibroblast growth factor receptors (FGFRs) are crucial in bone development and related

* Corresponding author. Department of Oral Histology-Developmental Biology, School of Dentistry and Dental Research Institute, Seoul National University, 1, Gwanak-ro, Gwanak-gu, Seoul, 08826, Republic of Korea.
** Corresponding author. Department of Oral Hygiene, Namseoul University, Cheonan, 31020, Republic of Korea.
E-mail addresses: bhs@nsu.ac.kr (H.S. Bae), iceburge@snu.ac.kr (D.-S. Lee).

https://doi.org/10.1016/j.heliyon.2025.e41789
Received 18 October 2024; Received in revised form 3 January 2025; Accepted 7 January 2025
Available online 8 January 2025

diseases. Numerous studies have demonstrated that FGFRs, particularly FGFR1, FGFR2, and FGFR3, are essential for regulating cranial suture development. FGFR1 is primarily found in osteoblasts and the mesenchymal tissue of the skull, where it is associated with the differentiation of osteoprogenitor cells. In contrast, FGFR2 is mainly expressed in proliferating osteogenic stem cells and regulates cell proliferation. Notably, before the differentiation of osteoprogenitor cells in the coronal sutures of mice, the expression of FGFR2 is downregulated while FGFR1 expression is upregulated [6–11]. These studies indicate that FGF signaling may be essential in cranial bone development.

NFI-C was first reported as a critical regulator in tooth development, particularly the formation of the tooth root, at a specific time during postnatal development [12–18]. Later, *Nfic*-deficient mice ($Nfic^{-/-}$ mice) had abnormalities in odontoblast proliferation and differentiation, resulting in abnormal incisors and short molar root formation [13–15]. It was reported that NFI-C acts downstream of the Runt-related transcription factor (Runx2), a transcription factor playing a central role in the development process of the teeth as well as bones, and upstream of another transcription factor, Osterix (Osx), and controls the formation of bones through the regulation of Osx [16]. Moreover, NFI-C was a critical factor in the proliferation of epiphyseal chondrocytes, a growth plate for long bones [17]. Additionally, we previously indicated that NFI-C is vital for maintaining the stem cell niche in mineralized tissues and may serve as an additional factor to improve reprogramming efficiency. We showed that *Nfic* regulates epithelial cell proliferation through epithelial-mesenchymal interactions in dental epithelial stem cells (DESCs), controlling the *Fgf8-Nfic-Sox2* pathway in the epithelium while the *Nfic-Fgf10* pathway in the mesenchyme [18]. However, the correlation between *Nfic* and *FGF* signaling in calvarial bone development is unclear.

Based on these previous findings, this study aims to determine the effects of *Nfic* on the proliferation of calvarial osteogenic progenitor cells and osteoblast differentiation in calvarial bone formation using *Nfic*-deficient mice and reveal the underlying molecular mechanism in this process. These findings suggest that *Nfic* plays an essential role in the proliferation and differentiation of calvarial osteogenic progenitors through regulating Fgfr1 during calvarial bone development.

2. Materials and methods

2.1. Reagents and antibodies

Rabbit cyclin D1 (2922), Fgfr1 (9740), Erk1/2 (9102), and p-Erk1/2 (4370) were obtained from Cell Signaling Technology. Antibodies against PCNA (sc-400), p21 (sc-6246), caspase-8 (sc-7890), and caspase-3 (sc-7148) were obtained from Santa Cruz Biotechnology, Inc.

2.2. Mice

Experiments involving mice were conducted following the guidelines of the Dental Research Institute and the Institutional Animal Care and Use Committee at Seoul National University (SNU-181127-13-2). $Nfic^{-/-}$ mice were generated by deleting the second exon of the *Nfic* gene. $Nfic^{-/-}$ mice were obtained by breeding heterozygous $Nfic^{+/-}$ mice. The genotypes of the mice were determined as previously described [12]. Due to the brittle teeth characteristic of $Nfic^{-/-}$ mice, a ground standard rodent chow was provided to all animals three times a week, starting three days before weaning and continuing for up to six weeks [16].

2.3. Micro-computed tomography (micro-CT) analysis, histology, and immunohistochemistry

The skulls of two and six weeks wild-type (WT) and *Nfic*-deficient mice were removed, fixed in 4 % paraformaldehyde at 4 °C overnight, and subjected to micro-CT using a SkyScan scanner and associated software (Skyscan 1172, Kontich, Belgium). The instrument's isotopic resolution is 10 μm. After reconstruction, we selected a round region of interest (ROI) around the midline suture (4 mm in diameter) for further quantitative analysis. BMD and BV/TV were measured using the CTan program.

Decalcified skulls were embedded in paraffin and cut into sections 5-μm thick. They were stained using hematoxylin-eosin (H&E) and then analyzed using immunohistochemistry (IHC) as previously described [16].

2.4. Skeletal analyses

The skulls of two- and four weeks were prepared and stained using Alcian blue for cartilage and alizarin red S for bone. First, the skin and internal organs were removed, and the skulls were fixed for five days in 95 % ethanol, followed by two days in acetone. The samples were stained for three days with a solution containing 0.015 % Alcian blue 8GX (Sigma) and 0.005 % alizarin red S (Sigma) in a mixture of 5 % glacial acetic acid and 70 % ethanol. After staining, the samples were treated with 80 % glycerol and ultimately stored in 100 %.

2.5. MTT assays

The proliferation rates of primary calvarial osteoprogenitor cells were assessed using MTT assays. The cells were seeded and cultured in 96-well plates at a density of 3000 cells per well. After washing with PBS, 50 μl of MTT solution (5 mg/ml) was added to each well, followed by an incubation period of 4 h at 37 °C. Once the incubation was complete, the MTT solution was removed, and the resulting dye was dissolved in DMSO. The absorbance at 540 nm was then measured using a microplate reader (Multiskan EX).

Triplicate samples from two independent experiments were analyzed.

2.6. Cell culture and transfection

Primary calvarial osteoprogenitor cells were isolated from the calvaria (parietal and frontal bones) of 7-day-old wild-type (WT) and *Nfic*$^{-/-}$ mice. In brief, the calvaria were harvested and dissected into fragments. These fragments were washed in phosphate-buffered saline (PBS), minced into several pieces, and digested for 1 h with 1 % Collagenase Type I (Gibco BRL) and 1.6 % Dispase II (Gibco BRL) in the alpha-MEM medium under an atmosphere containing 5 % CO_2. The cells were then cultured in alpha-MEM supplemented with 1x antibiotic antimycotic solution and 10 % fetal bovine serum (FBS). Human bone marrow stem cells (hBMSCs) were obtained from Lonza Pte. Ltd. (Cat. No. PT-2501) and cultured in low glucose DMEM supplemented with 1x antibiotic antimycotic solution and 10 % FBS.

For plasmid construction, a 0.56-kb genomic fragment was amplified from human genomic DNA to obtain the FGFR1 promoter region (−555 to +145). One microliter of human genomic DNA was subjected to PCR using the following cycling conditions: 94 °C for 1 min, 60 °C for 1 min, and 72 °C for 1 min for 35 cycles. The sense and anti-sense primers used were as follows: FGFR1 Sense: 5′-TCT CCG GTC CGA GCT CGG GGC GCC C-3′, FGFR1 Anti-sense: 5′-ACG AGC GCA GGG AGG GGG CGC AGG A-3′, FGFR1 Mutant Sense: 5′-GGG CGC GTC GTC CCG AGC GG-3′, and FGFR1 Mutant Anti-sense: 5′-CCG CTC GGG ACG ACG CGC CC-3'. The amplified fragment was then subcloned into the PCR®2.1 T vector and ligated into the *Xho*I and *Hin*dIII sites of the pGL3 luciferase (LUC) basic expression vector (Promega).

2.7. Reverse transcription-polymerase chain reaction (RT-PCR) and real-time PCR analyses

2 μg of total RNA was reverse transcribed using 0.5 μg of Oligo d(T) and one μL (50 IU) of Superscript III (Invitrogen) in a 20 μl reaction mixture at 50 °C for 1 h. The resulting cDNAs were amplified using PCR. Primers specific to *mNfic, mRunx2, mOsx, mAlp, mBsp, mOc, mDmp1, mFgfr1, mFgfr2, hFGFR1, hFGFR2, hNFI-C*, and *hGAPDH* were synthesized for real-time PCR (see Table 1).

2.8. Western blot analysis

Western blot analyses were executed precisely, following established protocols [16]. In brief, we separated 30 μg of total proteins using 10 % SDS-PAGE. Proteins were electrophoretically transferred to a nitrocellulose membrane (Schleicher & Schuell BioScience) and incubated with specific antibodies. Labeled proteins were then detected using an enhanced chemiluminescence system from GE Healthcare, ensuring the reliability of the results.

Table 1
Nucleotide sequences of real-time PCR primers.

Gene	Primer (5′-3′)	
mNfic	Forward	GACCTGTACCTGGCCTACTTTG
	Reverse	CACACCTGACGTGACAAAGCTC
Bsp	Forward	CAGGGAGGCAGTGACTCTTC
	Reverse	AGTGTGGAAAGTGTGGCGTT
mOc	Forward	CTGACAAAGCCTTCATGTCCAA
	Reverse	GCGCCGGAGTCTGTTCACTA
mAlp	Forward	CCAACTCTTTTGTGCCAGAGA
	Reverse	GGCTACATTGGTGTTGAGCTTTT
Runx2	Forward	TTCTCCAACCCACGAATGCAC
	Reverse	CAGGTACGTGTGGTAGTGAGT
mOsx	Forward	CCCACCCTTCCCTCACTCAT
	Reverse	CCTTGTACCACGAGCCATAGG
mFgfr1	Forward	TGTTTGACCGGATCTACACA
	Reverse	CTCCCACAAGAGCACTCCAA
mFgfr2	Forward	TCGCATTGGAGGCTATAAGG
	Reverse	CATTGATGGTGAGGTGTGCA
mGapdh	Forward	AGGTCGGTGTGAACGGATTTG
	Forward	TGTAGACCATGTAGTTGAGGTCA
hFGFR1	Forward	AACCTGACCACAGAATTGGA
	Reverse	ATGCTGCCGTACTCATTCTCC
hFGFR2	Forward	TGATGGACTTCCTTATGTCCG
	Reverse	AGCGTCCTCTTCTGTGACATT
hNFIC	Forward	CGACTTCCAGGAGAGCTTTG
	Reverse	GTTCAGGTCGTATGCCAGGT
hGAPDH	Forward	CCATGGAGAAGGCTGGGG
	Reverse	CAAAGTTCTCATGGATGACC

2.9. ChIP assays

ChIP assays were conducted as previously described [16]. hBMSCs were transiently transfected with an NFI-C expression plasmid for 48 h. The samples were then sonicated, followed by chromatin immunoprecipitation using 30 μl of anti-NFIC antibodies and 10 μl of anti-IgG antibodies (Santa Cruz). The final DNA pellets were recovered and analyzed by polymerase chain reaction (PCR) using specific primers, as listed in Table 2. The PCR conditions were set as follows: 94 °C for 30 s, 60 °C for 30 s, and 72 °C for 30 s for 35 cycles. The PCR products were analyzed using electrophoresis on a 2 % agarose gel.

2.10. Statistical analysis

All quantitative data are presented as means ± standard deviation (SD) using SPSS 26. The significance of differences was assessed with a Student's t-test (*P < .05, **P < .01, ***P < .001).

3. Results

3.1. Evaluation of mice calvaria formation by Nfic gene targeting

The calvaria of two-week-old (P14) and four-week-old (P28) mice, both WT and *Nfic*-deficient, were removed, and calvaria formation was analyzed using micro-CT and Alizarin Red S and Alcian Blue staining to evaluate the effect of the absence of *Nfic* on the calvaria formation. The micro-CT analysis of 2-week-old mice showed that the nasal bone of mice deficient in the *Nfic* gene was observed to be different from that of wild-type mice, and the density of the nasal bone was also reduced (Fig. 1A). Comparing the calvaria of WT and *Nfic*-deficient mice using Alizarin Red S and Alcian Blue staining, the calvaria of both 2-week-old and 4-week-old mice of the *Nfic*-deficient mice showed a delay in the fusion of the interfrontal suture. In contrast, the calvaria of 4-week-old mice of the *Nfic*-deficient mice was abnormal, with deformation pointing toward the right compared to WT mice (Fig. 1B). In micro-CT analyses, *Nfic*-deficient mice exhibited significant decreases in bone volume (BV/TV, 36 %) and bone mineral density (BMD, 14 %) but no change in bone thickness (Tb. Th) (Fig. 1C). We also identified males and females by histology and found no sex differences regarding reduced trabecular bone density and increased trabecular bone separation. However, we used only male littermates for all the experiments to reduce variation.

3.2. Evaluation of bone formation in mice with Nfic gene targeting

The calvaria of six-week-old mice, both WT and deficient in *Nfic*, were removed, and calvaria formation was compared using micro-CT analysis to confirm the effects of *Nfic*'s absence on skull formation. The micro-CT analysis of 6-week-old mice showed that the basisphenoid bone of the skull of *Nfic*-deficient mice was diagnosed with osteoporosis. In contrast, the sagittal suture was diagnosed with interrupted suture closure compared to WT mice (Fig. 2A). Using 3D micro-CT analysis, *Nfic*-deficient mice had reduced calvaria bone volume (BV/TV, 33 %), bone thickness (Tb. Th, 16 %), and bone mineral density (BMD, 23.5 %) compared to WT mice at a statistically significant level (Fig. 2B). Through histological analysis, it was observed that the calvaria of *Nfic*-deficient mice had a delay in the sagittal suture closure and a reduction in thickness compared to those of WT mice (Fig. 2C).

3.3. Effects of Nfic gene absence on osteoblast differentiation

Osteoprogenitor cells were isolated from WT and *Nfic*-deficient mice's calvaria and investigated for their ability to differentiate into osteoblasts. ALP staining on day 7 of differentiation and Alizarin Red S (ARS) on day 14 showed that *Nfic*-deficient osteoprogenitor cells had lower ALP activation and reduced calcified nodules. ALP activity and quantity of ARS staining in *Nfic* deficiency calvarial osteoprogenitor cells decreased approximately five-fold compared to WT cells (Fig. 3A). These results show that the NFI-C plays an essential role in the differentiation process of osteoblasts. Real-time polymerase chain reaction (PCR) was used on day 7 of differentiation to examine the WT and *Nfic*-deficient osteoprogenitor cells for osteoblast-specific gene expression. The expression of transcription factor *Runx2*, which regulates osteoblast differentiation, showed no difference in WT and *Nfic*-deficient osteoprogenitor cells, but *Osx* expression was reduced by about 5-fold in osteoprogenitor cells deficient in the *Nfic* gene (Fig. 3B and C). The gene expressions of *Alp*, osteocalcin (*Oc*), *Bsp*, and *Dmp1*, all osteoblasts marker genes, were also significantly reduced in osteoprogenitor cells deficient in the *Nfic* gene (Fig. 3D–G). These results showed that the *Nfic* acting downstream of *Runx2* regulated *Osx* expression, which also regulated osteoblast differentiation.

Table 2
Nucleotide sequences of ChIP assay PCR primers.

Gene	Primer (5′-3′)	
hFGFR1 promoter P1	Forward (−198)	ACACGCCCGCTCGCACAAGC
	Reverse (−50)	GCAAAGCGCGCAGCCGGGA
hFGFR1 promoter P2	Forward (−483)	GGGGCCTCCGCAGGGCGATG
	Reverse (−335)	GCCGGAGCTGGTGCCCCGGA

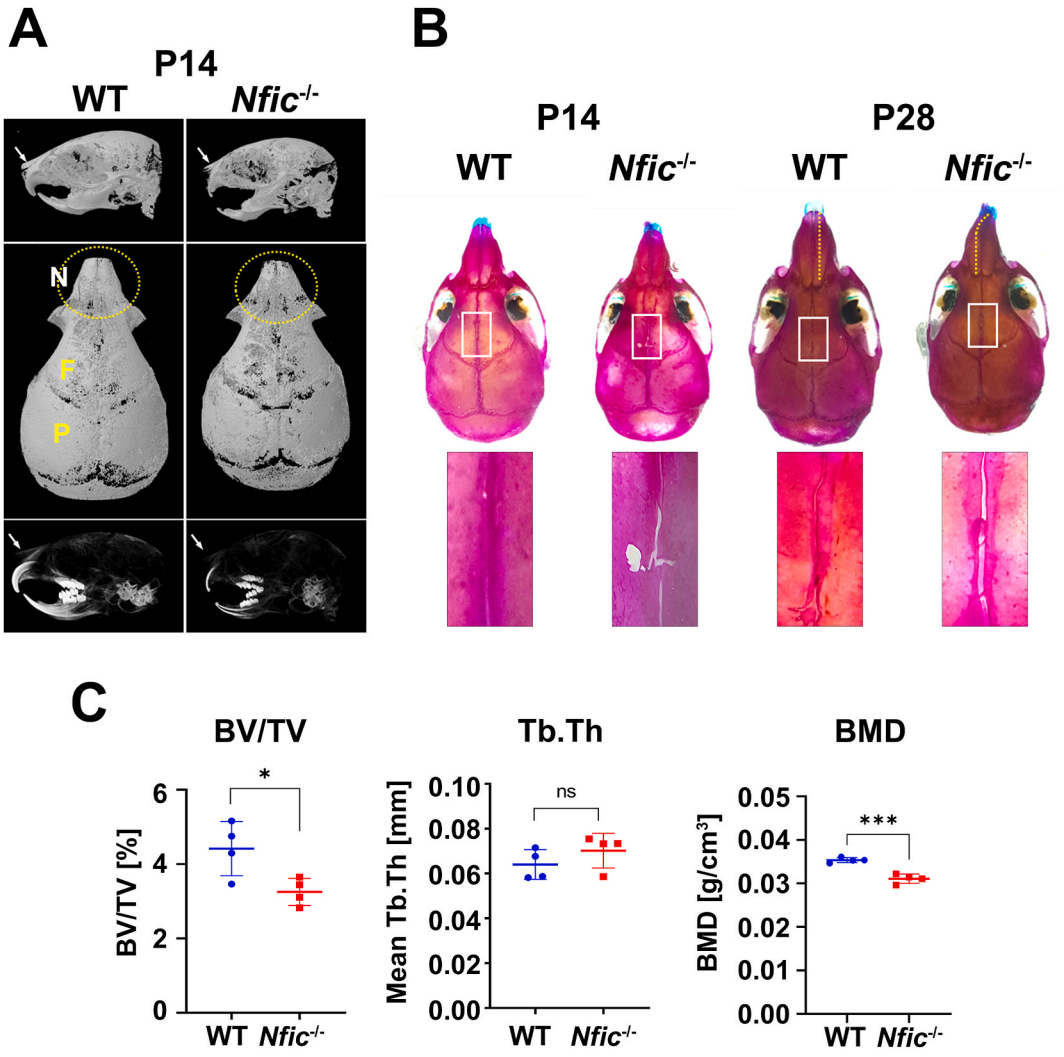

Fig. 1. Defect of calvarial ossification in *Nfic*-deficient mice **(A)** Representative micro-CT image of the calvarial bone in wild-type (WT) and *Nfic*-deficient mice at P14. White arrows (top and bottom panels) and yellow dotted circles (middle panels) represent the nasal bone. **(B)** The skull in WT and *Nfic*-deficient mice was analyzed using Alizarin red S and Alcian blue staining at P14 and P28. Yellow dotted lines are marked along the contour of the nasal bone. The area of the interfrontal suture is boxed in the upper panels and shown at higher magnification in the lower panels. N, nasal bone; F, frontal bone; P, parietal bone. **(C)** Micro-CT quantification of the calvarial bone in WT and *Nfic*-deficient mice at P14. Calvarial bone volume, BV/TV (%); Calvarial bone thickness, Mean Tb.Th (mm). Calvarial bone mineral density, BMD (g/cm^3). n = 4, *, $p < .05$, ***, $p < .001$. ns, no significance.

3.4. Effects of Nfic on osteoprogenitor cell proliferation and apoptosis

Cell proliferation in WT mice and *Nfic*-deficient mice sutures was observed to investigate the cellular mechanism underlying defective suture closure in mice deficient in the *Nfic* gene. The cell proliferation marker gene PCNA from wild-type and *Nfic*-deficient mice was immunohistochemically stained, and these results showed that while cells stained with PCNA antibodies were observed in mice deficient in the gene, the cells stained with the PCNA antibodies in the sutures of *Nfic*-deficient mice were decreased about fivefold compared to WT mice (Fig. 4A).

Osteoprogenitor cells were isolated from the calvaria of WT and *Nfic*-deficient mice, and an MTT assay was performed to confirm cell proliferation in vitro. The results of the MTT assay revealed that *Nfic* deficiency significantly reduced cell proliferation of osteoprogenitor cells from day 3 of cell culture compared to WT (Fig. 4B). Furthermore, in osteoprogenitor cells deficient in *Nfic*, the protein level of Cyclin D, which promotes the cell cycle process, was reduced. In contrast, the protein level of p21, which is a factor that suppresses the cell cycle process, increased (Fig. 4C).

Next, the protein levels of Caspase-8 and Caspase-3, which play a central role in cell apoptosis, were compared between the osteoprogenitor cells of WT mice and *Nfic*-deficient mice using Western blot to investigate the effects of *Nfic* absence on osteoprogenitor cells in their apoptosis. Generally, the level of caspase-8 in its cleaved form, known as the initiator caspase, was higher in

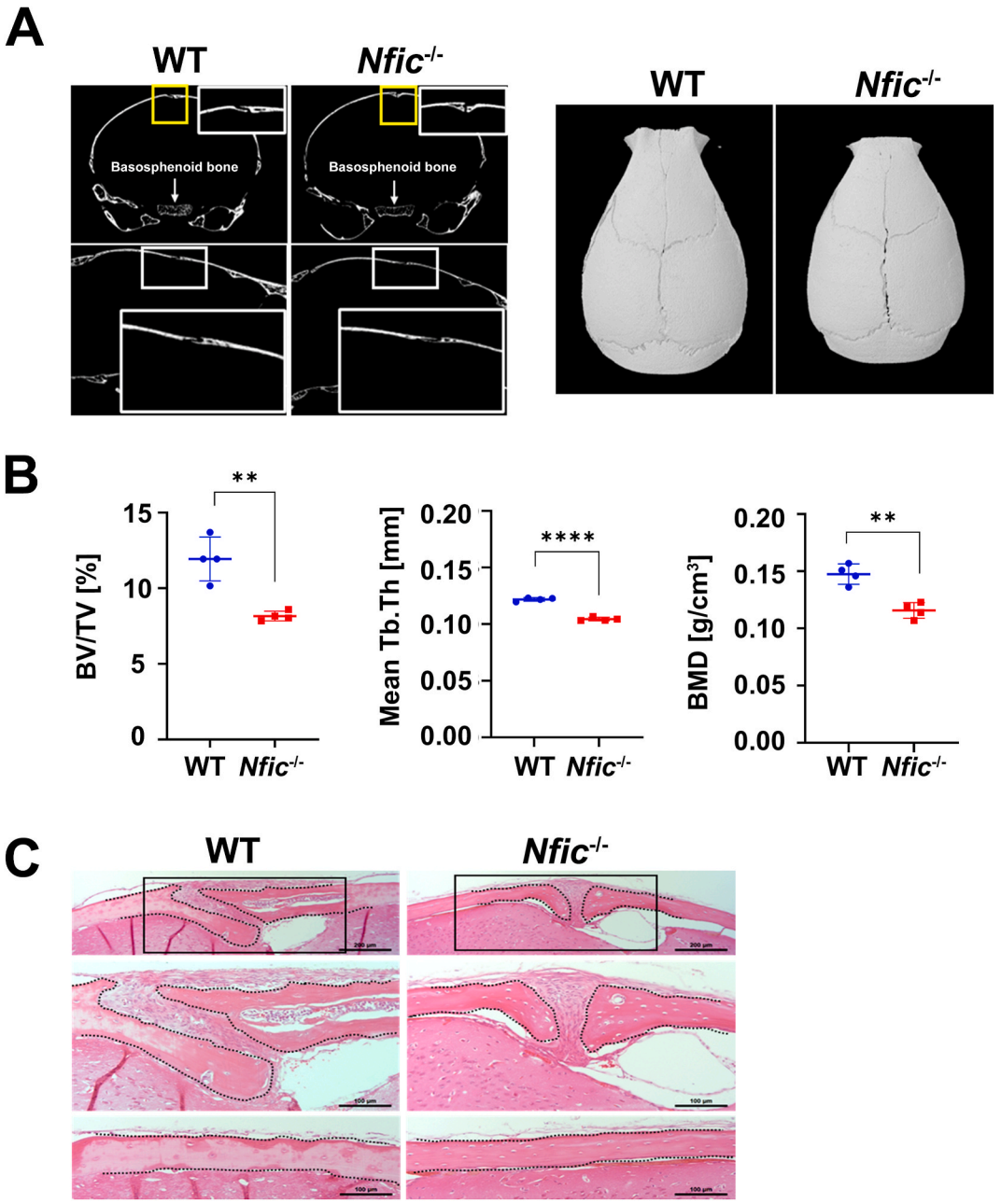

Fig. 2. Impaired calvarial bone formation during postnatal osteogenesis in *Nfic*-deficient mice **(A)** Micro-CT slices showing the sagittal sutures in wild-type (WT) and *Nfic*-deficient mice at 6 weeks. Basisphenoid bone in the *Nfic*-deficient mice shows lower bone density (arrow) compared with the WT (upper panels). Micro-CT slices showing coronal sutures in WT and *Nfic*-deficient mice (lower panels). Yellow rectangles in the upper panels are shown at higher magnification in the upper right and lower panels. **(B)** 3D micro-CT images of calvarial bone at 6 weeks. Micro-CT quantification of calvarial bone. Calvarial bone volume, BV/TV (%); Calvarial bone thickness, Mean Tb.Th (mm). Calvarial bone mineral density, BMD (g/cm^3). Data are presented as the mean ± S.D. (n = 4, **, $p < .01$, ****, $p < .0001$). **(C)** H&E staining of histological sections from the calvarial bone in WT and *Nfic*-deficient mice at 6 weeks. Middle panels are sagittal sutures of calvarial bone. Lower panels are calvarial bone. Middle panels are higher magnifications of the boxed upper panels. Scale bars, middle panel, 200 μm; Middle and lower panels, 100 μm.

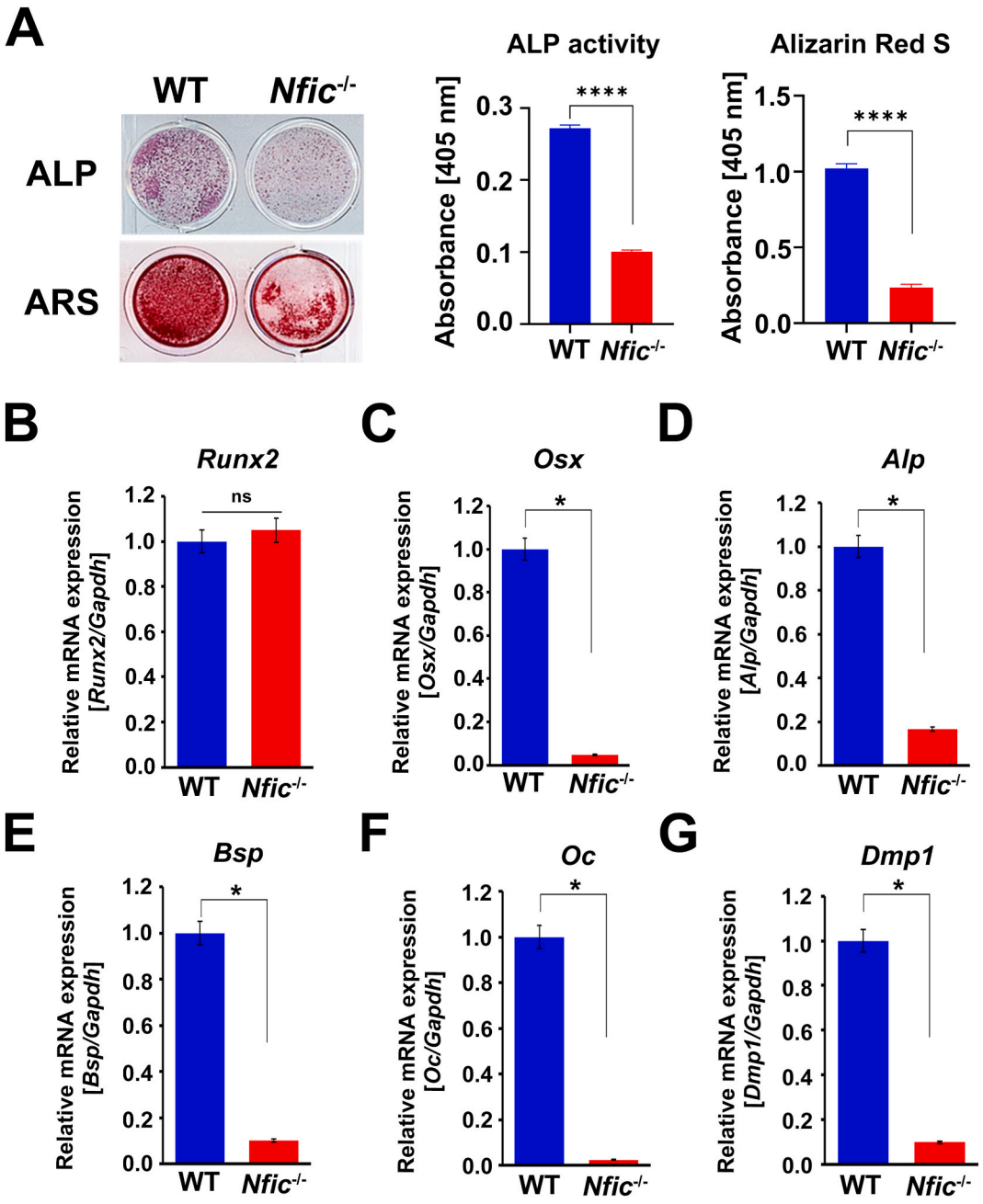

Fig. 3. Impaired osteoblast differentiation in *Nfic*-deficient mice (**A**) Alkaline phosphatase (ALP) and alizarin red S (ARS) staining in WT and *Nfic*-deficient calvarial osteoblasts and activity. WT and *Nfic*-deficient calvarial osteoprogenitor cells were cultured in osteogenic induction media for 7 days and analyzed using ALP staining. WT and *Nfic*-deficient calvarial osteoprogenitor cells were cultured in osteogenic induction media for 14 days and analyzed by ARS staining. Expression of (**B**) *Runx2*, (**C**) *Osx*, (**D**) *ALP*, (**E**) *Bsp*, (**F**) *OC*, and (**G**) *Dmp1* was analyzed using real-time PCR in WT and *Nfic*-deficient calvarial osteoprogenitor cells after differentiation for 7 days. $n = 3$; *p < .05. Data are presented as the mean ± S.D.

osteoprogenitor cells deficient in *Nfic* than in WT (Fig. 4D). Active caspase-8 cleaves procaspase-3 and promotes its activity, leading to apoptosis. Procasepase-3 and cleaved caspase-3 levels were higher in *Nfic*-deficient osteoprogenitor cells (Fig. 4E).

3.5. Fibroblast growth factor receptor 1 (Fgfr1) and Fgfr2 gene expressions in osteoprogenitor cells of Nfic gene-targeted mice

Fgfr1 and *Fgfr2* expressions in osteoprogenitor cells were observed to investigate the relevance of the *Fgf* gene family in abnormal calvaria formation of *Nfic*-deficient mice. *Fgfr1* and *Fgfr2* gene expressions in osteoprogenitor cells deficient in the *Nfic* gene were

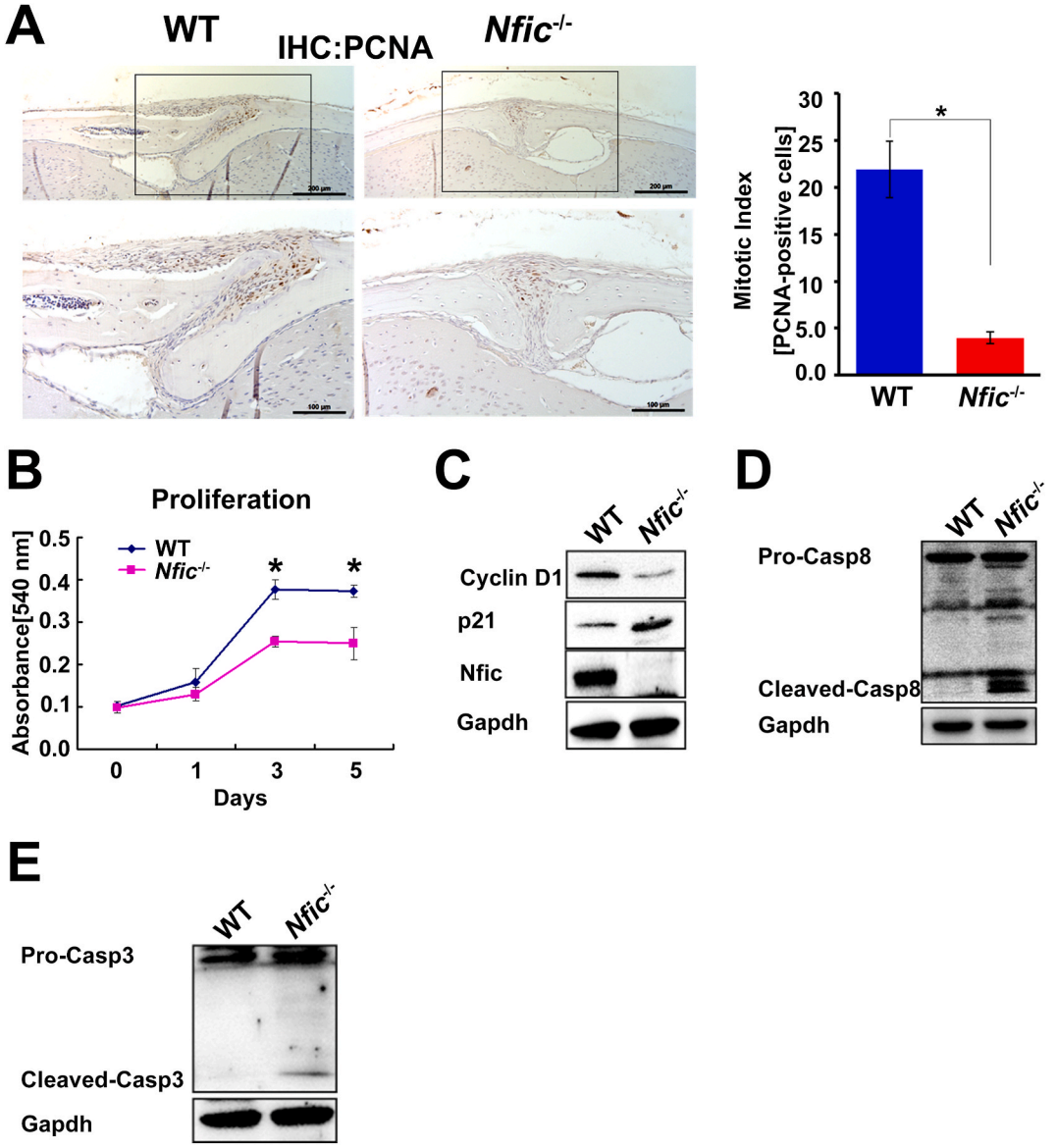

Fig. 4. Reduced osteogenic cell Proliferation in *Nfic*-deficient calvaria (**A**) PCNA immunostaining was performed in 6-week-old calvaria from WT and *Nfic*-deficient mice using the PCNA antibody. Lower panels have higher magnifications than boxed upper panels. Scale bars, upper panels, 200 μm; lower panels, 100 μm. (**B**) Primary calvarial osteoprogenitor cells isolated from calvaria from WT and *Nfic*-deficient mice at ages P3∼5. Calvarial osteoprogenitor cells were seeded on 96-well plates at 3×10^3 cells/well density. Cell proliferation was measured using MTT assays at 0, 1, 3, and 5 days. Data are presented as the mean ± S.D. ($n = 3$, $^*p < .05$). (**C**) Cyclin D1, p21, and *Nfic* expression were detected in cell lysates using western blotting. (**D**) Caspase-8 and (**E**) Caspase3 expression were detected in cell lysates using western blotting. Glyceralaldehyde-3-phosphate dehydrogenase (GAPDH) served as an internal control. (see Supplemental Fig.s4C-E).

observed to be reduced by 2.5-fold and 2-fold, respectively, compared to WT (Fig. 5A and B). Furthermore, the *Fgfr1* protein expression was also reduced in osteoprogenitor cells deficient in the *Nfic* gene (Fig. 5C). The ERK/MAPK cascade has been demonstrated to be an important intracellular mediator of FGF signaling [10]. Therefore, we investigated the activity of ERK in calvarial osteoprogenitor cells from WT and nfic deficient mice. Activated ERK1/2 was significantly reduced in *Nfic* deficient calvarial osteoprogenitor cells compared with WT (Fig. 5C).

3.6. *Effects of the NFI-C gene on the expression of FGFR1*

The *NFI-C* gene was overexpressed in human-derived mesenchymal stem cells, following which *FGFR1* and *FGFR2* mRNA expressions were observed using real-time PCR to verify the effects of *NFI-C* on regulating *Fgfr1* expression. *NFI-C* gene expression was

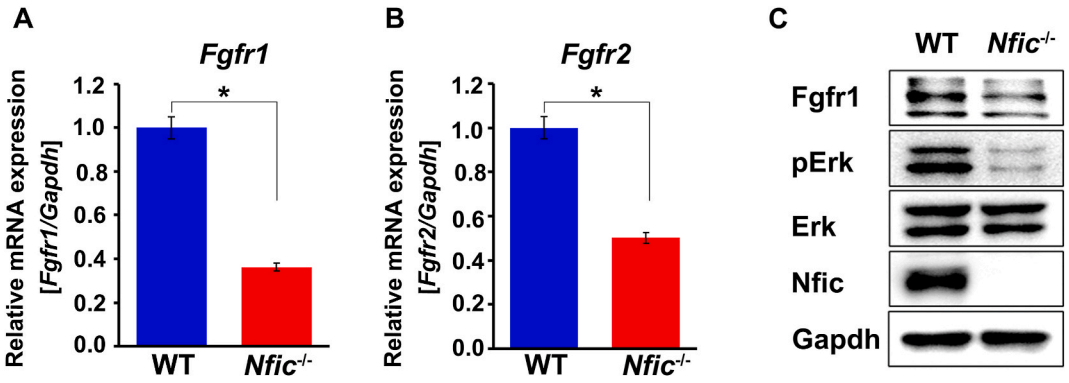

Fig. 5. Effects of *Nfic* disruption on *Fgf* gene family expression in the WT and *Nfic* $^{-/-}$ calvarial osteoblasts. Primary calvarial osteoprogenitor cells are isolated from calvaria from WT and *Nfic*-deficient mice at ages postnatal day 3~5. Calvarial osteoprogenitor cells were seeded on 60 mm culture dishes at 2.5×10^5 cells/dish density. (**A**) *FGFR1* and (**B**) *FGFR2* mRNA expression levels were analyzed using real-time PCR. (**C**) Western blotting detected Fgfr1, pErk, Erk, and Nfic protein levels in WT and *Nfic*-deficient calvarial osteoprogenitor cell lysates. Data are presented as the mean ± S. D. (n = 3, *p < .05). (see Supplemental Fig.s5B).

increased by around 550-fold (Fig. 6A), while the *FGFR1* and *FGFR2* expressions increased by around 5 times and 3.5 times, respectively, due to *NFI-C* overexpression (Fig. 6B and C). Western blot was used to assess the FGFR1 protein expression, and the results showed that the FGFR1 protein expression was also increased in mesenchymal stem cells with overexpressed NFI-C, while phosphorylation of ERK acting downstream of the FGF signaling pathway was also found to increase (Fig. 6D). Next, the NFI binding motif of FGFR1's promoter region was investigated to determine whether *NFI-C* directly regulated *FGFR1* expression. The NFI binding motif was identified within positions −198 and −50 of the *FGFR1* promoter region sequence, and the human-derived mesenchymal stem cells were overexpressed with the *NFI-C* gene, followed by a ChIP assay for verification. From the ChIP assay, NFI-C protein binding was not observed in the FGFR1 promoter region that does not contain the NFI binding motif (P2), but NFI-C protein binding was observed in the FGFR1 promoter region with the NFI binding motif (P1) (Fig. 6E). In addition, NFI-C binds to its specific DNA binding site in the FGFR1 promoter (Fig. 6E). When the NFI-C binding motif in the FGFR1 promoter was mutated, NFI-C could not enhance the activity of the FGFR1 promoter (Fig. 6F). These data indicate that NFI-C is positioned upstream in the NFIC-FGFR1 signaling pathway.

4. Discussion

This study investigated the effects of the transcription factor *Nfic* on calvarial osteogenic progenitor cell proliferation and differentiation from the standpoint of the *Runx2-Nfic-Osx* and *Runx2-Nfic-Fgf* signaling pathways.

Runx2 is part of the Runx family and the essential transcription factor in skeletal development. Runx2 is necessary for the proliferation of osteoprogenitor cells and osteoblast differentiation, and bone formation cannot proceed without Runx2. Furthermore, Runx2 induces Osx expression in preosteoblasts, leading to these cells' differentiation into osteoblasts [19]. According to a study by Lee et al. [16], if NFI-C acting downstream from Runx2 is disrupted in the bone marrow, osteogenesis in the bone marrow is decreased, and adipogenesis increases and this is considered a result of the inability of *Osx* to act downstream of *Nfic* to be expressed resulting in relatively higher adipocytes within the bone marrow. In this study, the *Nfic* disruption did not affect *Runx2* expression, but *Osx* expression was suppressed, and osteoblast differentiation was disrupted, leading to reduced calvarial bone length and density abnormalities. The study results revealed that *Nfic* regulates bone formation via the *Runx2-Nfic-Osx* signaling pathway, which acts on the intermediary stage of *Runx2* and *Osx* in calvaria in the same manner as in the bone marrow. These results also suggest that if *Nfic* is targeted in calvaria, the upstream factor *Runx2* is unaffected. In contrast, through regulation of the downstream factor *Osx*, the later stages of osteoblast differentiation could be selectively regulated, and *Nfic* could thus be effectively utilized in the prevention and treatment of calvaria formation diseases.

Since the *Fgf* gene family plays an essential role in the proliferation and differentiation of osteoblasts in the development of bone, numerous studies have reported that the defective *Fgf* gene expression in calvaria leads to deformities in calvarial bone development and formation [3–5]. The premature fusion of the cranial suture, an essential factor in defective cranial bone development, is modulated by basic *Fgf* and *Fgfr* [5,20]. *Fgfr1* and *Fgfr2* are expressed in osteoprogenitor cells and regulate cranial osteoblast phenotype, osteoblast function, osteoblast, and osteocyte death and growth [21,22]. More recently, it was revealed that *Runx2* regulated *Fgfr2* and *Fgfr3* expressions and modulated osteoprogenitor cell proliferation [23–25]. Moreover, FGF signaling plays an essential role during tooth development. We previously demonstrated that Nfic regulates FGF10 expression in the dental mesenchyme in mouse incisors. In addition, Nfic is activated through FGF8 signaling in dental epithelial tissues to regulate stem cell capacity and cell proliferation of these tissues [18]. Here, we showed that *Nfic* regulates the proliferation of calvarial osteoprogenitor cells through modulation of *FGFR1* expression. In addition, we identified that the expression of *FGF1* and *FGF2* was reduced in calvarial osteoprogenitor cells of *Nfic*-deficient mice (data not shown).

Interestingly, the ChIP assay revealed that FGFR1 functioned by binding to NFI-C. Additionally, when *Nfic* is disrupted, *Fgfr1* and *Fgfr2* expressions are suppressed, while conversely, *NFI-C* overexpression in hBMSCs results in increased *FGFR1* and *FGFR2*

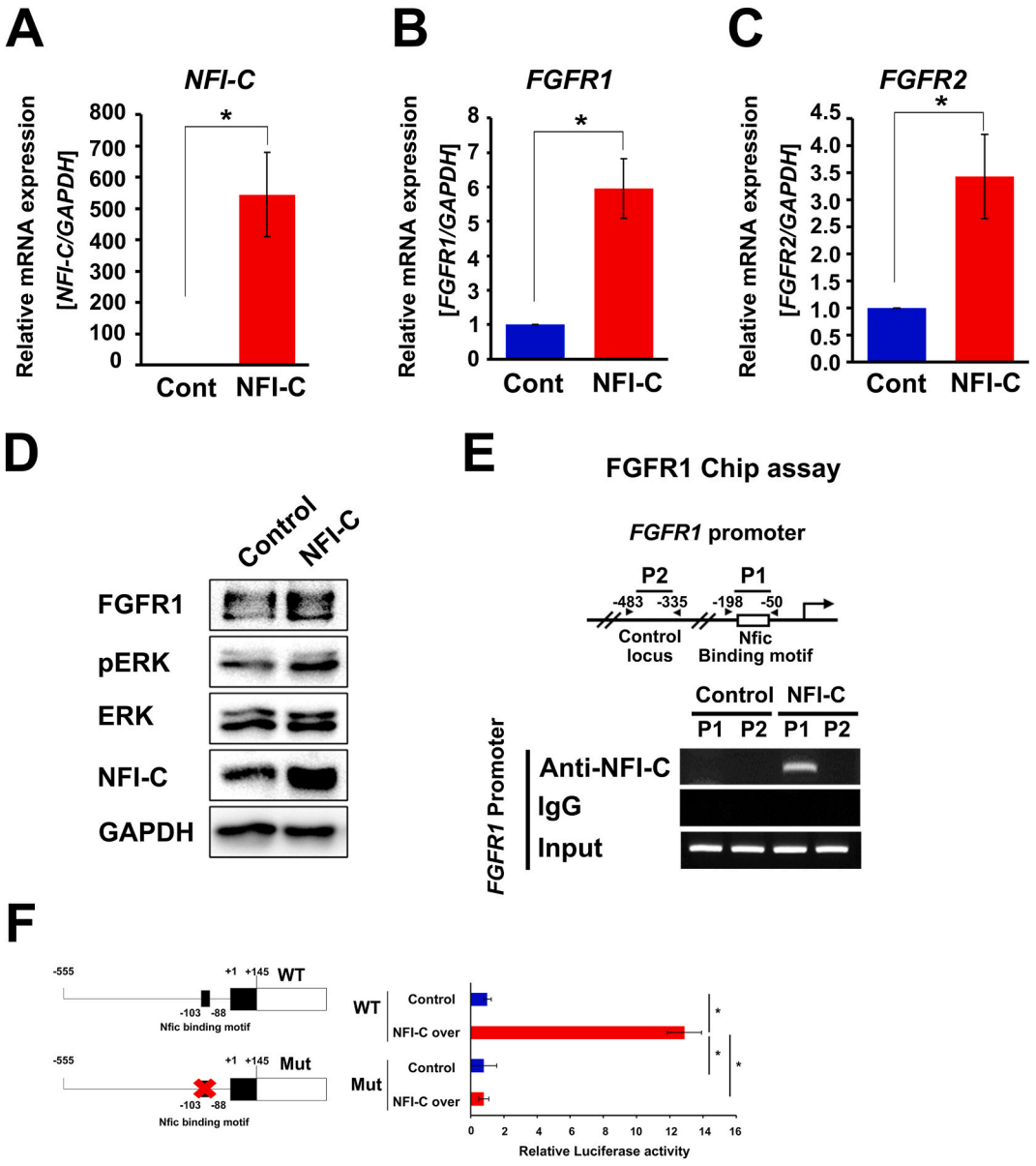

Fig. 6. Effects of NFI-C on FGFR1 and FGFR2 gene expression in the hBMSCs.Expression of Real-time PCR and Western blot analyses to determine the level of (**A**) *NFI-C*, (**B**) *FGFR1*, and (**C**) *FGFR2* expression in human bone marrow stem cells (BMSCs) transfected with NFI-C expression vectors. Data are presented as the mean ± S.D. (n = 3, *p < .05). (**D**) Western blotting detected FGFR1, pErk, Erk, and NFI-C expression in cell lysates. (**E**) NFI-C binding to the FGFR1 promoter was detected using ChIP analyses in hBMSCs transfected with NFI-C expression vectors. (**F**) Schematic representation of FGFR1 promoters and the deletion of the NFI-C binding motif. The effect of NFI-C on the FGFR1 promoter activity in the presence and/or absence of the NFI-C binding motif is shown. FGFR1 promoter activity was assessed in MC3T3-E1 cells transfected with pGL3-Luc-FGFR1 and pGL3-Luc-FGFR1 Mutation constructs in the presence of NFI-C for 48 hr. n = 5, *p < .05. (see Supplemental Fig.s 6D and E)

expressions. In addition, when evaluating the effect of *NFI-C* on FGFR1 promoter activity, *NFI-C* increased FGFR1 promoter activity, but when the NFI binding motif was mutated in the FGFR1 prompter, it did not increase FGFR1 promoter activity. These results revealed that the *NFI-C* regulated *FGFR1* and *FGFR2* expressions via *NFIC-FGF* signaling pathway irrespective of *Osx*, resulting in calvarial osteoprogenitor cell proliferation modulation. Nonetheless, further research is needed to investigate the direct relevance between *NFI-C* and *FGFR2* and whether *NFI-C* binds to the *FGFR2* gene and regulates transcription and translation.

Xingwen Wang et al. recently reported that miR-34a regulates osteoblast proliferation and apoptosis through FGFR1 [23]. These results indicate the importance of FGFR1 in osteoblast proliferation and apoptosis. In addition, several studies have shown that the ERK MAPK pathway, a downstream factor of FGFR, increases osteoblast differentiation and bone formation in vitro and *in vivo* [24–26]. Furthermore, mice lacking Erk1 and Erk2 in the limb and head mesenchyme (Erk1 $^{-/-}$ Erk2 Prx1) exhibited severe limb malformations

and impaired skeletal mineralization [27,28]. Therefore, these reports support our findings that the absence of *Nfic* causes defects in the FGFR1-Erk signaling pathway, leading to decreased cell proliferation and increased apoptosis in calvarial osteoprogenitor cells [29].

p21 suppresses the activity of cyclin E/CDK2, cyclin D1/CDK4/6, cyclin A/CDK2, and so on, allowing cell growth to remain at the G1/S checkpoint, resulting in suppression of cell proliferation through inhibition of the cell cycle [30,31]. This study showed that *Nfic* disruption increased the expression of p21 in calvarial osteoprogenitor cells. In turn, this reduced the expression of Cyclin D1, disrupting cell proliferation and relatively increased expression of cleaved-Caspase8 and cleaved-Caspase3 overall, leading to cell apoptosis. This suggests that, as opposed to *Nfic* disruption, calvarial osteoprogenitor cell proliferation could be induced by *Nfic* overexpression, thus regulating osteoblast differentiation and calvarial bone formation.

In conclusion, this study revealed that the transcription factor *Nfic* regulates the cell proliferation of calvarial osteogenic progenitor cells via the *Nfic-Fgf* signaling pathway and the differentiation of calvarial osteogenic progenitor cells via the *Nfic-Osx* signaling pathway. The study results point toward further research on utilizing *Nfic* to prevent calvaria diseases such as craniosynostosis due to defective cell proliferation and differentiation of osteogenic progenitor cells.

CRediT authorship contribution statement

Jieun Lee: Writing – original draft, Investigation, Conceptualization. **Joo-Cheol Park:** Writing – review & editing, Data curation, Conceptualization. **Heung-Joong Kim:** Data curation, Conceptualization. **Hyun Sook Bae:** Writing – review & editing, Data curation, Conceptualization. **Dong-Seol Lee:** Writing – review & editing, Data curation, Conceptualization.

Ethics approval and consent to participate

This study was reviewed and approved by the Institutional Animal Care and Use Committee of Seoul National University with the approval number [SNU-181127-13-2]

Data availability statement

All data generated and analyzed during this study are included in this article. Requests for this information can be made to the corresponding author.

Declaration of competing interest

The authors declare that they have no known competing financial interests or personal relationships that could have appeared to influence the work reported in this paper.

Acknowledgments and Funding

This work was supported by the National Research Foundation of Korea (NRF) grant, which was funded by the Korea government, Republic of Korea (No. NRF-2021R1A2C1095165).

Appendix A. Supplementary data

Supplementary data to this article can be found online at https://doi.org/10.1016/j.heliyon.2025.e41789.

References

[1] L.A. Opperman, Cranial sutures as intramembranous bone growth sites, Dev Dyn 219 (2000) 472–485, https://doi.org/10.1002/1097-0177.
[2] R.S. Tubbs, A.N. Bosmia, A.A. Cohen-Gadol, The human calvaria: a review of embryology, anatomy, pathology, and molecular development, Childs Nerv Syst. 28 (1) (2012) 23–31, https://doi.org/10.1007/s00381-011-1637-0.
[3] H. Zhao, J. Feng, T.V. Ho, W. Grimes, M. Urata, Y. Chai, The suture provides a niche for mesenchymal stem cells of craniofacial bones, Nat. Cell Biol. 17 (4) (2015) 386–396, https://doi.org/10.1038/ncb3139.
[4] S.M. Warren, L.J. Brunet, R.M. Harland, A.N. Economides, M.T. Longaker, The BMP antagonist noggin regulates cranial suture fusion, Nature 10 (422) (2003) 625–629, https://doi.org/10.1038/nature01545, 6932.
[5] M.S. Raam, B.D. Solomon, S.A. Shalev, M. Muenke, Holoprosencephaly and craniosynostosis: a report of two siblings and review of the literature, Am J Med Genet C Semin Med Genet 15 (1) (2010) 176–182, https://doi.org/10.1002/ajmg.c.30234, 154C.
[6] Xiaolei Zhao, Erhardt Shannon, Kihan Sung, Jun Wang, FGF signaling in cranial suture development and related diseases, Front. Cell Dev. Biol. 11 (2023) 1112890, https://doi.org/10.3389/fcell.2023.1112890.
[7] Chad M. Teven, Evan M. Farina, Jane Rivas, R Reid Russell, Fibroblast growth factor (FGF) signaling in development and skeletal diseases, Genes Dis 1 (2) (2014) 199–213, https://doi.org/10.1016/j.gendis.2014.09.005.
[8] S. Zhu, W. Chen, A. Masson, Y.P. Li, Cell signaling and transcriptional regulation of osteoblast lineage commitment, differentiation, bone formation, and homeostasis, Cell Discov 10 (71) (2024), https://doi.org/10.1038/s41421-024-00689-6.

[9] X. Zhao, S. Erhardt, K. Sung, J. Wang, FGF signaling in cranial suture development and related diseases, Front. Cell Dev. Biol. 11 (2023) 1112890, https://doi.org/10.3389/fcell.2023.1112890.
[10] D.M. Roth, K. Souter, D. Graf, Craniofacial sutures: signaling centres integrating mechanosensation, cell signaling, and cell differentiation, Eur. J. Cell Biol. 101 (2022) 151258, https://doi.org/10.1016/j.ejcb.2022.151258.
[11] Amr M. Moursi, Phillip L. Winnard, Alissa V. Winnard, John M. Rubenstrunk, Mark P. Mooney, Fibroblast growth factor 2 induces increased calvarial osteoblast proliferation and cranial suture fusion, Cleft Palate Craniofac J 39 (5) (2002) 487–496, https://doi.org/10.1597/1545-1569_2002_039_0487_fgfiic_2.0.co_2.
[12] G. Steele-Perkins, K.G. Butz, G.E. Lyons, M. Zeichner-David, H.J. Kim, M.I. Cho, R.M. Gronostajski, Essential role for NFI-C/CTF transcription-replication factor in tooth root development, Mol. Cell Biol. 23 (3) (2003) 1075–1084, https://doi.org/10.1128/MCB.23.3.1075-1084.2003.
[13] J.C. Park, Y. Herr, H.J. Kim, R.M. Gronostajski, M.I. Cho, Nfic gene disruption inhibits differentiation of odontoblasts responsible for root formation and results in formation of short and abnormal roots in mice, J. Periodontol. 78 (9) (2007) 1795–1802, https://doi.org/10.1902/jop.2007.060363.
[14] T.Y. Lee, D.S. Lee, H.M. Kim, J.S. Ko, R.M. Gronostajski, M.I. Cho, H.H. Son, J.C. Park, Disruption of nfic causes dissociation of odontoblasts by interfering with the formation of intercellular junctions and aberrant odontoblast differentiation, J. Histochem. Cytochem. 57 (5) (2009) 469–476, https://doi.org/10.1369/jhc.2009.952622.
[15] D.S. Lee, J.T. Park, H.M. Kim, J.S. Ko, H.H. Son, R.M. Gronostajski, M.I. Cho, P.H. Choung, J.C. Park, Nuclear factor I-C is essential for odontogenic cell proliferation and odontoblast differentiation during tooth root development, J. Biol. Chem. 19 (25) (2009) 17293–17303, https://doi.org/10.1074/jbc.M109.009084, 284.
[16] D.S. Lee, H.W. Choung, H.J. Kim, R.M. Gronostajski, Y.I. Yang, H.M. Ryoo, Z.H. Lee, H.H. Kim, E.S. Cho, J.C. Park, NFI-C regulates osteoblast differentiation via control of osterix expression, Stem Cell. 32 (9) (2014) 2467–2479, https://doi.org/10.1002/stem.1733.
[17] D.S. Lee, S.Y. Roh, H. Choi, J.C. Park, NFI-C is required for epiphyseal chondrocyte proliferation during postnatal cartilage development, Mol Cells 43 (8) (2020) 739–748, https://doi.org/10.14348/molcells.2020.2272.
[18] Dong-Seol Lee, Yeo Joon Song, Hye Ri Gug, Ji-Hyun Lee, Hyun Sook Bae, Joo-Cheol Park, Nuclear factor I-C regulates stemness genes and proliferation of stem cells in various mineralized tissue through epithelial-mesenchymal interactions in dental epithelial stem cells, Stem Cells Int (2022) 1092184, https://doi.org/10.1155/2022/1092184.
[19] T. Komori, Molecular mechanism of runx2-dependent bone development, Mol Cells 29 (2) (2020) 168–175, https://doi.org/10.14348/molcells.2019.0244, 43.
[20] D.M. Ornitz, P.J. Marie, Fibroblast growth factors in skeletal development, Curr. Top. Dev. Biol. 133 (2019) 195–234, https://doi.org/10.1016/bs.ctdb.2018.11.020.
[21] M. Kawai, D. Herrmann, A. Fuchs, S. Cheng, A. Ferrer-Vaquer, R. Gotz, K. Driller, A. Neubuser, K. Ohura, Fgfr1 conditional-knockout in neural crest cells induces heterotopic chondrogenesis and osteogenesis in mouse frontal bones, Med. Mol. Morphol. 52 (2019) 156–163, https://doi.org/10.1007/s00795-018-0213-z.
[22] J.A. Greenwald, B.J. Mehrara, J.A. Spector, S.M. Warren, P.J. Fagenholz, L.E. Smith, P.J. Bouletreau, F.E. Crisera, H. Ueno, M.T. Longaker, In vivo modulation of FGF biological activity alters cranial suture fate, Am. J. Pathol. 158 (2) (2001) 441–452, https://doi.org/10.1016/s0002-9440(10)63987-9.
[23] X. Wang, J. He, H. Wang, D. Zhao, B. Geng, S. Wang, J. An, C. Wang, H. Han, Y. Xia, Fluid shear stress regulates osteoblast proliferation and apoptosis via the lncRNA TUG1/miR-34a/FGFR1 axis, J. Cell Mol. Med. 25 (2021) 8734–8747. https://10.1111/jcmm.16829.
[24] M. Kawai, D. Herrmann, A. Fuchs, S. Cheng, A. Ferrer-Vaquer, R. Gotz, K. Driller, A. Neubuser, K. Ohura, Fgfr1 conditional-knockout in neural crest cells induces heterotopic chondrogenesis and osteogenesis in mouse frontal bones, Med. Mol. Morphol. 52 (2019) 156–163. https://10.1007/s00795-018-0213-z.
[25] M.B. Greenblatt, J.H. Shim, S. Bok, J.M. Kim, The extracellular signal-regulated kinase mitogen-activated protein kinase pathway in osteoblasts, J Bone Metab 29 (2022) 1–15. https://10.11005/jbm.2022.29.1.1.
[26] A. De Simone, M.N. Evanitsky, L. Hayden, B.D. Cox, J. Wang, V.A. Tornini, J. Ou, A. Chao, K.D. Poss, S. Di Talia, Control of osteoblast regeneration by a train of Erk activity waves, Nature 590 (2021) 129–133. https://10.1038/s41586-020-03085-8.
[27] M.R. Hasan, M. Takatalo, H. Ma, R. Rice, T. Mustonen, D.P. Rice, RAB23 coordinates early osteogenesis by repressing FGF10-pERK1/2 and GLI1, Elife 9 (2020). https://10.7554/eLife.55829.
[28] J.M. Kim, Y.S. Yang, K.H. Park, H. Oh, M.B. Greenblatt, J.H. Shim, The ERK MAPK pathway is essential for skeletal development and homeostasis, Int. J. Mol. Sci. 20 (2019), https://doi.org/10.3390/ijms20081803.
[29] T. Matsushita, Y.Y. Chan, A. Kawanami, G. Balmes, G.E. Landreth, S. Murakami, Extracellular signal-regulated kinase 1 (ERK1) and ERK2 play essential roles in osteoblast differentiation and in supporting osteoclastogenesis, Mol. Cell Biol. 29 (2009) 5843–5857. https://10.1128/MCB.01549-08.
[30] R.E. Shackelford, W.K. Kaufmann, R.S. Paules, Oxidative stress and cell cycle checkpoint function, Free Radic. Biol. Med. 28 (9) (2000) 1387–1404, https://doi.org/10.1016/s0891-5849(00)00224-0.
[31] S.J. Park, S.J. Kim, Y. Rhee, J.H. Byun, S.H. Kim, M.H. Kim, E.J. Lee, S.K. Lim, Fidgetin-like 1 gene inhibited by basic fibroblast growth factor regulates the proliferation and differentiation of osteoblasts, J. Bone Miner. Res. 22 (2007) 889–896. https://10.1359/jbmr.070311.